



HAL
open science

Possible structural quantum criticality tuned by rare-earth ion substitution in infinite-layer nickelates

Alaska Subedi

► **To cite this version:**

Alaska Subedi. Possible structural quantum criticality tuned by rare-earth ion substitution in infinite-layer nickelates. 2022. hal-03850463

HAL Id: hal-03850463

<https://hal.science/hal-03850463v1>

Preprint submitted on 27 Nov 2022

HAL is a multi-disciplinary open access archive for the deposit and dissemination of scientific research documents, whether they are published or not. The documents may come from teaching and research institutions in France or abroad, or from public or private research centers.

L'archive ouverte pluridisciplinaire **HAL**, est destinée au dépôt et à la diffusion de documents scientifiques de niveau recherche, publiés ou non, émanant des établissements d'enseignement et de recherche français ou étrangers, des laboratoires publics ou privés.

Possible structural quantum criticality tuned by rare-earth ion substitution in infinite-layer nickelates

Alaska Subedi

CPHT, CNRS, Ecole Polytechnique, IP Paris, F-91128 Palaiseau, France

(Dated: April 12, 2022)

Materials with competing phases that have similar ground state energies often exhibit a complex phase diagram. Cuprates are a paradigmatic example of such a system that show competition between charge, magnetic, and superconducting orders. The infinite-layer nickelates have recently been revealed to feature similar characteristics. In this paper, I show that these nickelates are additionally near a structural quantum critical point by mapping the energetics of their structural instabilities using first principles calculations. I first confirm previous results that show a phonon instability in the $P4/mmm$ phase leading to the $I4/mcm$ structure for $RNiO_2$ with $R = \text{Sm-Lu}$. I then study the non-spin-polarized phonon dispersions of the $I4/mcm$ phase and find that they exhibit rare-earth size dependent instabilities at the X and M points for materials with $R = \text{Eu-Lu}$. Group-theoretical analysis was used to enumerate all the isotropy subgroups due to these instabilities, and the distorted structures corresponding to their order parameters were generated using the eigenvectors of the unstable phonons. These structures were then fully relaxed by minimizing both the atomic forces and lattice stresses. I was able to stabilize only five out of the twelve possible distortions. The $Pbcn$ isotropy subgroup with the $M_5^+(a, a)$ order parameter shows noticeable energy gain relative to other distortions for the compounds with late rare-earth ions. However, the order parameter of the lowest-energy phase switches first to $X_2^-(0, a) + M_5^+(b, 0)$ and then to $X_2^-(0, a)$ as the size of the rare-earth ion is progressively increased. Additionally, several distorted structures lie close in energy for the early members of this series. These features of the structural energetics persist even when antiferromagnetism is allowed. Such a competition between different order parameters that can be tuned by rare-earth ion substitution suggests that any structural transition that could arise from the phonon instabilities present in these materials can be suppressed to 0 K.

INTRODUCTION

The recent report of superconductivity in thin films of $\text{Nd}_{0.8}\text{Sr}_{0.2}\text{NiO}_2$ by Li *et al.* has rekindled interest in the infinite-layer nickelates because the nominal valence of Ni^{1+} in these materials has the same $3d^9$ electronic configuration with $s = \frac{1}{2}$ that is found in the Cu^{2+} ions of the cuprates [1]. Subsequently, signatures of superconductivity have also been found in thin films of doped PrNiO_2 and LaNiO_2 [2–4]. A large amount of experimental [5–41] and theoretical [42–82] effort has already been expended in understanding the electronic and magnetic properties of these materials. However, the microscopic mechanism underlying the observed superconductivity has not been fully clarified.

One reason for the lack of progress in this direction is the absence of full chemical and structural information of the samples that exhibit superconductivity, which stems from the difficulty in performing diffraction experiments on thin films. It is also not well understood how the sample growth conditions affect the chemical and structural factors that give rise to superconductivity in these materials. For example, superconductivity has not yet been observed in polycrystalline powders with the same chemical composition as that of the superconducting thin films [6, 12]. Furthermore, superconductivity seems to be observed in thin films of only around 10 nm in thickness [1, 4, 13, 21, 23]. Interestingly, density functional theory (DFT) calculations show that the stoichiometric

compound is thermodynamically unstable, with hydrogenation reducing this instability [74, 83].

In any case, experimental probes have so far been oblivious to any presence of hydrogen in the superconducting thin films, and the two-dimensional layers formed by NiO_4 squares have been thought to be the key structural ingredient behind the superconductivity in these materials. DFT calculations show that the parent compound NdNiO_2 hosting these layers is stable, but the calculated electron-phonon coupling is too small to account for the observed T_c [46]. Calculations that utilize the DFT electronic structure and take into account the many-body effects find a $d_{x^2-y^2}$ -wave superconducting instability, which has strengthened the case for an unconventional nature of superconductivity in these materials [43, 45, 62]. Such an order parameter would exhibit nodes in the superconducting order parameter. Currently, there is experimental support for both nodal and nodeless superconducting gap [38, 40].

There is also experimental evidence for structural instability in these materials. Polycrystalline powders and single crystals of these materials have been refined to the tetragonal $P4/mmm$ structure [29, 84–87]. Recent resonant x-ray scattering experiments, however, find a charge order near the wave vector $(\frac{1}{3}, 0)$ in lightly-doped LaNiO_2 and NdNiO_2 thin films [34–36]. DFT-based phonon dispersions calculations do not find any structural instabilities in these two materials, but they do show the $P4/mmm$ structure to be dynamically unstable for the

infinite-layer nickelates with smaller rare-earth ions [77–80].

In this paper, I extend previous studies of the structural instabilities in the infinite-layer nickelates presented in Refs. [77–80] by investigating the instabilities that were not considered in these works. I first calculate the non-spin-polarized phonon dispersions of all $P4/mmm$ $R\text{NiO}_2$ compounds with $R = \text{La-Lu}$ (including Y also as a rare-earth element) and reproduce previous results that find a phonon instability at the $A (\frac{1}{2}, \frac{1}{2}, \frac{1}{2})$ point for $R = \text{Sm-Lu}$. This instability leads to an $I4/mcm$ structure that exhibits in-plane rotation of the NiO_4 squares that is out-of-phase in the out-of-plane direction.

I then go beyond the previous studies by calculating the non-spin-polarized phonon dispersions of this phase for the compounds with $R = \text{Sm-Lu}$. I find only SmNiO_2 to be stable in the $I4/mcm$ structure. The $I4/mcm$ phase of GdNiO_2 exhibits an instability at the $X (\frac{1}{2}, \frac{1}{2}, 0)$ point, while the compounds with $R = \text{Gd-Lu}$ exhibit an additional instability at the $M (0, 0, 1)$ point. I used group-theoretical analysis to identify all the twelve different distortions that are possible due to these instabilities. Only five of these distorted structures could be stabilized after full structural relaxations minimizing both the atomic forces and lattice stresses. While the $Pbcn$ structure with the order parameter $M_5^+(a, a)$ exhibits significant energy gain relative to other distortions for the compounds with late rare-earth elements, several distorted structures lie close in energy in the early members of this series. Moreover, among the nearly degenerate structures, the order parameter of the lowest-energy distortion changes first to $X_2^-(0, a) + M_5^+(b, 0)$ and then to $X_2^-(0, a)$ as the size of the rare-earth ion is progressively increased. These aspects of the structural energetics remain even in the antiferromagnetic state. This presence of competing structural phases arising out of phonon instabilities that can be tuned by rare-earth ion substitution suggests that the infinite-layer nickelates lie in the vicinity of a structural quantum critical point.

COMPUTATIONAL APPROACH

The phonon calculations presented here were obtained using density functional perturbation theory as implemented in the QUANTUM ESPRESSO package [88, 89]. This is a pseudopotential-based code, and I used the pseudopotentials generated by Dal Corso [90]. The calculations were performed within the generalized gradient approximation of Perdew, Burke and Ernzerhof (PBE) [91] using planewave cutoffs of 60 and 600 Ry, respectively, for the basis-set and charge density expansions. The Brillouin zone integration was performed using $16 \times 16 \times 16$, $12 \times 12 \times 12$, and $12 \times 12 \times 8$ k -point grids for the $P4/mmm$, $I4/mcm$, and $Pbcn$ phases, respectively. The dynamical matrices were obtained on

$8 \times 8 \times 8$, $4 \times 4 \times 4$, and $6 \times 6 \times 4$ q -point grids for the $P4/mmm$, $I4/mcm$, $Pbcn$ phases, respectively. A 0.008 Ry Marzari-Vanderbilt smearing was used in all the calculations.

I used the ISOTROPY package to determine all the order parameters that are possible due to the unstable phonon modes [92]. The distortions corresponding to these order parameters were then generated by utilizing the eigenvectors of the unstable phonon modes on 64-atom $2 \times 2 \times 2$ supercells of the primitive $I4/mcm$ unit cells. These structures were then fully relaxed by minimizing both the atomic forces and lattice stresses using the VASP package, which is a planewave implementation of the projector-augmented-wave method [93]. A planewave cutoff of 600 eV, k -point grid of $8 \times 8 \times 8$, and Methfessel-Paxton smearing of 0.1 eV were used in these calculations. A magnetic solution was not allowed. However, the fully relaxed structures were utilized to construct the conventional unit cells that allowed for a nearest-neighbor (G-type) antiferromagnetic ordering. These structures were again relaxed allowing for such an antiferromagnetic solution using equivalent or denser k -point grids. Some non-spin-polarized and magnetic structural relaxations were also performed on the $Pbnm a^-a^-c^+$ distortion of the $P4/mmm$ structure generated on 32-atom $2 \times 2 \times 2$ supercells. A planewave cutoff of 650 eV and k -point grid of $8 \times 8 \times 8$ were used in these calculations. Each component of the force is less than 1 meV/Å in the relaxed structures.

The spin-orbit interaction was neglected in all the calculations. The pseudopotentials of the rare-earth ions have the $4f$ electrons in the core such that the ions have a formal valence of 3+. I made extensive use of the FINDSYM [94], AMPLIMODES, and SPGLIB [95] packages in the symmetry analysis of the relaxed structures.

RESULTS AND DISCUSSION

Dynamical instability in the parent $P4/mmm$ phase

The calculated non-spin-polarized phonon dispersions of $R\text{NiO}_2$ in the $P4/mmm$ phase are given in Fig. 1 for $R = \text{Sm, Y, and Lu}$, which broadly agree with previous results [77, 78, 80]. The dispersions exhibit a nondegenerate phonon branch that is unstable at $A (\frac{1}{2}, \frac{1}{2}, \frac{1}{2})$. As noted by Xia *et al.*, this instability has a strong dependence on the rare-earth ion size [77]. The calculated frequency of the unstable mode at A as a function of the rare-earth ion is shown in Fig. 2. This mode is stable for compounds with large rare-earth ions La–Pm but becomes unstable for those with rare-earth ions Sm–Lu that have smaller ionic radii. The instability is quite weak for SmNiO_2 , with a calculated value of $26i \text{ cm}^{-1}$ for the imaginary frequency of the unstable mode. For LuNiO_2 , which has the smallest rare-earth ion, the instability is

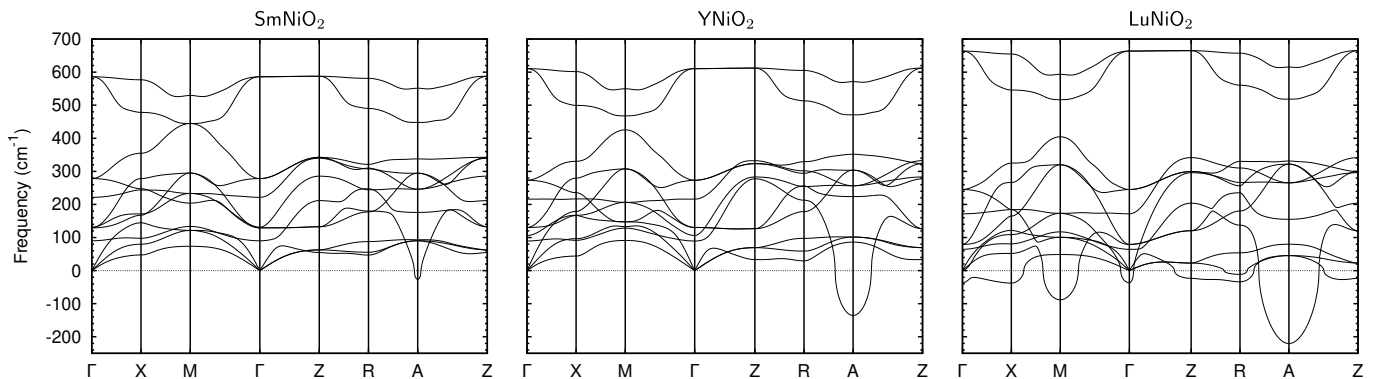


FIG. 1. Calculated non-spin-polarized phonon dispersions of fully-relaxed SmNiO_2 , YNiO_2 , and LuNiO_2 in the $P4/mmm$ phase. The high-symmetry points are Γ $(0, 0, 0)$, X $(0, \frac{1}{2}, 0)$, M $(\frac{1}{2}, \frac{1}{2}, 0)$, Z $(0, 0, \frac{1}{2})$, R $(0, \frac{1}{2}, \frac{1}{2})$, and A $(\frac{1}{2}, \frac{1}{2}, \frac{1}{2})$ in terms of the reciprocal lattice vectors. Imaginary frequencies are indicated by negative values.

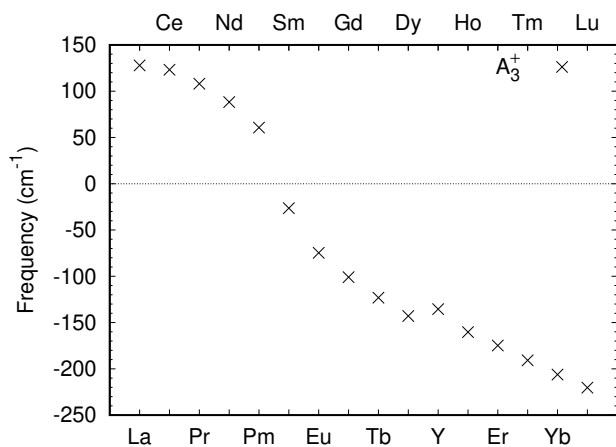


FIG. 2. Calculated phonon frequency of the A_3^+ mode of $R\text{NiO}_2$ (R = rare-earth) compounds in the non-spin-polarized $P4/mmm$ phase as a function of the rare-earth ions, which are sorted according to their ionic radii. Imaginary frequencies are indicated by negative values.

relatively strong with a calculated imaginary frequency of $220i \text{ cm}^{-1}$.

The instability at A causes an in-plane rotation of the NiO_4 squares that is out-of-phase along the c axis [77, 78]. With the convention that the Ni ion is at the origin, this mode has the irreducible representation (irrep) A_3^+ [78]. Since this mode is nondegenerate and A has only one element in its star, this instability leads to only one distorted structure. Group-theoretical analysis shows that this low-symmetry structure has the space group $I4/mcm$ [77–80].

I used the eigenvector of the unstable A_3^+ mode to generate the $I4/mcm$ structure for all the $R\text{NiO}_2$ compounds and fully relaxed the structure by minimizing both the atomic forces and lattice stresses. As expected, the $I4/mcm$ structure is lower in energy than the corresponding $P4/mmm$ structure only for those compounds that

exhibit an instability of the A_3^+ mode in the $P4/mmm$ phase (*i.e.* $R = \text{Sm–Lu}$), which is consistent with previous studies [77, 80]. The calculated energy gain range from relatively tiny 2.0 meV/atom for SmNiO_2 to noticeably large 74.3 meV/atom for LuNiO_2 .

Is the $I4/mcm$ phase stable?

I studied the structural stability of the $I4/mcm$ phase of the infinite layer rare-earth nickelates obtained above for $R = \text{Sm–Lu}$ by calculating their non-spin-polarized phonon dispersions, which are shown in Fig. 3 for SmNiO_2 , YNiO_2 , and LuNiO_2 . Fig. 4 shows the frequencies of the lowest-energy phonon modes at the X $(\frac{1}{2}, \frac{1}{2}, 0)$ and M $(0, 0, 1)$ points in their Brillouin zone for the compounds with $R = \text{Sm–Lu}$. I find that only SmNiO_2 is dynamically stable in the $I4/mcm$ phase. All other compounds exhibit phonon instabilities that are again strongly dependent on the rare-earth ion size. EuNiO_2 exhibits an instability only at the X point. Compounds with smaller rare-earth ions exhibit instabilities at both X and M . There is only one unstable mode at M for $R = \text{Gd–Er}$, while an additional unstable mode at M appears for smaller rare-earth ions Tm–Lu . Moreover, yet another instability at N appears for compounds with rare-earth ions from Ho to Lu . It is also noteworthy that the highly-dispersive soft branch between Γ – M shows a relatively small rare-earth size dependence. Interestingly, the lowest-frequency unstable modes at X , M , and N are all connected to unstable acoustic branches at Γ , which should manifest as a softening of the corresponding elastic moduli in experiments.

As can be seen in Fig. 4, the instability at X is larger than at M in all the $I4/mcm$ phases that exhibit these instabilities. The calculated difference of the imaginary frequencies between these modes is $9i \text{ cm}^{-1}$ for GdNiO_2 , which is the first member of this series that exhibits both these instabilities. As the size of the rare-earth ion is

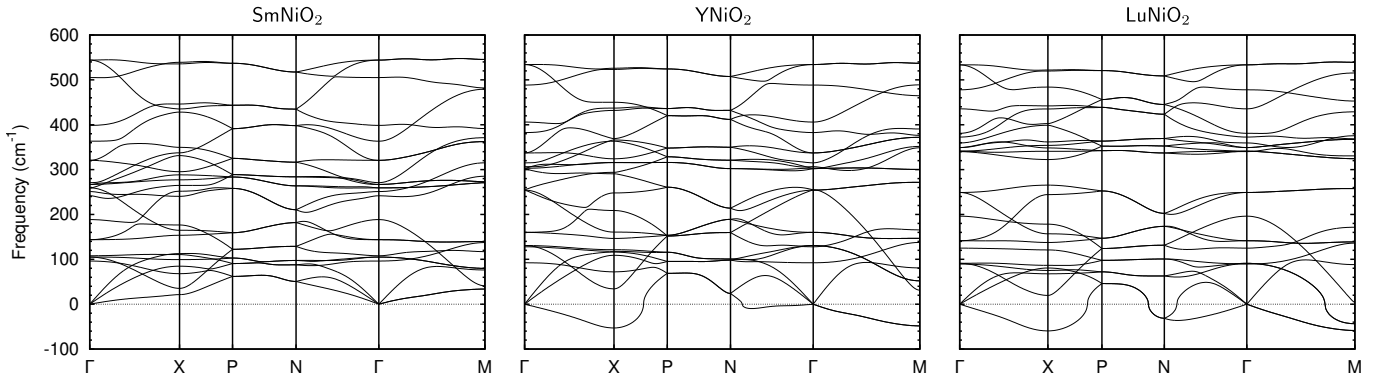


FIG. 3. Calculated non-spin-polarized phonon dispersions of fully-relaxed SmNiO_2 , YNiO_2 , and LuNiO_2 in the high-symmetry $I4/mcm$ phase. The high-symmetry points are Γ $(0, 0, 0)$, X $(\frac{1}{2}, \frac{1}{2}, 0)$, P $(\frac{1}{2}, \frac{1}{2}, \frac{1}{2})$, N $(\frac{1}{2}, 0, \frac{1}{2})$, and M $(0, 0, 1)$ in terms of the reciprocal lattice vectors of the conventional unit cell. Imaginary frequencies are indicated by negative values.

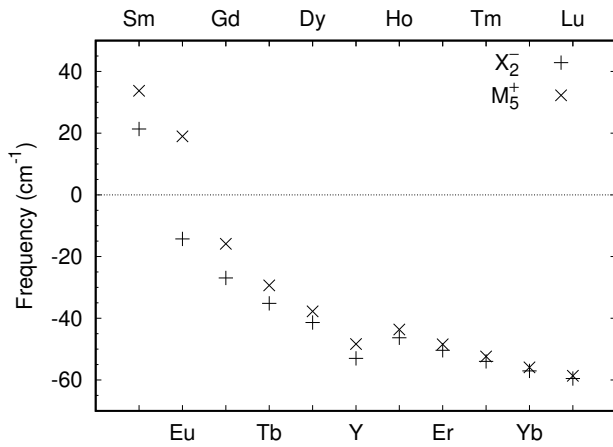


FIG. 4. Calculated phonon frequency of the X_2^- and M_5^+ modes of $R\text{NiO}_2$ ($R = \text{Sm–Lu}$ and Y) compounds in the non-spin-polarized $I4/mcm$ phase as a function of the rare-earth ions. Imaginary frequencies are indicated by negative values.

decreased, this difference decreases, and the instabilities at X and M become almost degenerate. For LuNiO_2 , the instabilities at X and M have imaginary frequencies of $59.5i$ and $58.6i$ cm^{-1} , respectively.

The unstable phonon mode at X in the $I4/mcm$ phase has the irrep X_2^- when the convention that one of the Ni ion is at the origin is used. This mode is nondegenerate, but the order parameter described by this instability is two dimensional because the star of X has two elements $\{(\frac{1}{2}, \frac{1}{2}, 0), (\frac{1}{2}, -\frac{1}{2}, 0)\}$. The atomic displacements resulting from this instability are shown in Fig. 5(b). A comparison with the undistorted $I4/mcm$ structure in Fig. 5(a) shows that the X_2^- mode causes an in-plane shear distortion of the R squares that is out-of-phase along the c axis. Additionally, the O-Ni-O bonds that are perpendicular to the direction of the displacement of R ions shift and buckle in the out-of-plane direction. The shift and buckling are out-of-phase along the

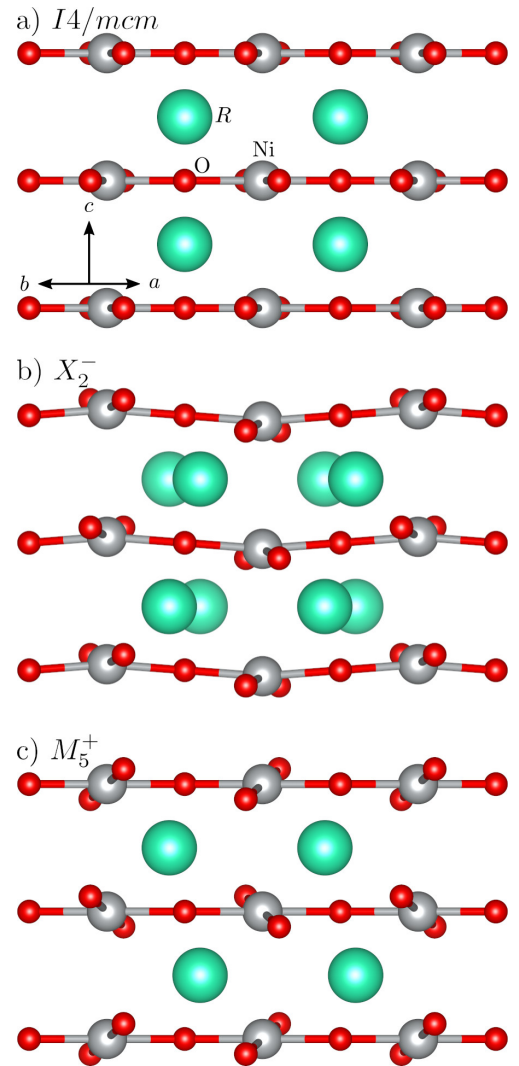


FIG. 5. a) $I4/mcm$ structure of the infinite-layer $R\text{NiO}_2$ compounds. Atomic displacements due to b) X_2^- and c) M_5^+ phonon instabilities of the $I4/mcm$ phase. The structures are projected along the in-plane diagonal direction.

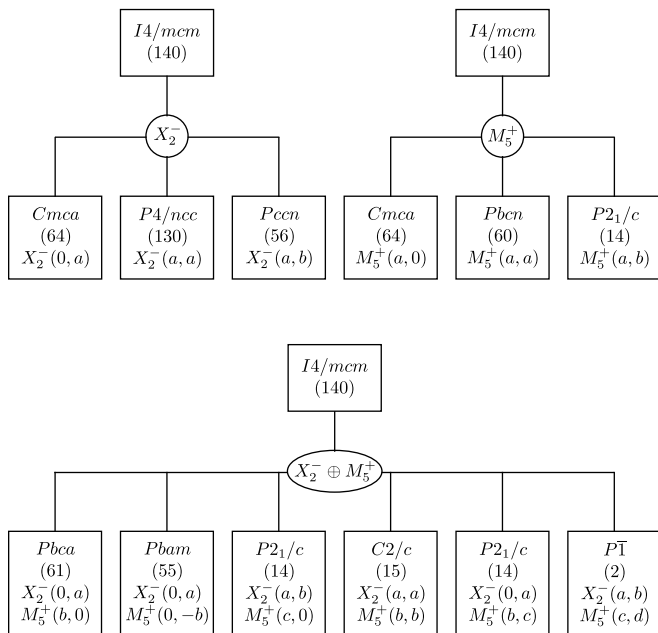


FIG. 6. Isotropy subgroups and the corresponding order parameters of the X_2^- and M_5^+ irreps of the $I4/mcm$ space group. The space group numbers are given in the parenthesis.

displacement direction of the R ions, but in-phase along the c axis.

The lowest-frequency unstable mode at M has the irrep M_5^+ . This mode is doubly degenerate and the star of M has only one element. So the order parameter due to this instability is also two dimensional. Fig. 5(c) shows the atomic displacements caused by this mode, which involves a sliding of the R planes that is out-of-phase along the c axis. There is also an out-of-plane tilting of the NiO_4 squares that is out-of-phase along the sliding direction of the R planes and in-phase along the c axis.

Which low-symmetry structures derive from the phonon instabilities of the $I4/mcm$ phase ?

I used group-theoretical analysis to identify all the distortions that can arise due to the X_2^- and M_5^+ instabilities. These irreps each have three isotropy subgroups. In addition, there are six subgroups due to the coupling of the X_2^- and M_5^+ order parameters. The order parameters and space groups of all the low-symmetry structures that can arise due to these two instabilities are shown in Fig. 6. I used the eigenvectors of these unstable phonon modes to generate the twelve distortions of the $I4/mcm$ phase in its 64-atom $2 \times 2 \times 2$ supercell for the compounds with $R = \text{Eu-Lu}$. These were then fully relaxed by minimizing both the atomic forces and lattice stresses without allowing for a magnetic solution. Out of twelve possible distortions, only five could be stabilized. They

TABLE I. Total energies of the five isotropy subgroups of the X_2^- and M_5^+ instabilities present in the $I4/mcm$ phase of the $R\text{NiO}_2$ compounds that could be stabilized using non-spin-polarized DFT calculations. The energies are given relative to the respective $I4/mcm$ phase in the units of meV/atom. Note that the order parameters refer to that of the initial structures. Symmetry-allowed distortions appear for the final relaxed structures. Only two distortions could be stabilized for EuNiO_2 .

	<i>Cmca</i>	<i>P4/ncc</i>	<i>Cmca</i>	<i>Pbcn</i>	<i>Pbca</i>
	$X_2^-(0, a)$	$X_2^-(a, a)$	$M_5^+(a, 0)$	$M_5^+(a, a)$	$X_2^-(0, a)$ + $M_5^+(b, 0)$
$R\text{NiO}_2$	$X_2^-(0, a)$	$X_2^-(a, a)$	$M_5^+(a, 0)$	$M_5^+(a, a)$	
Eu	< -0.1	< -0.1			
Gd	-2.8	-2.1	< -0.1	< -0.1	-2.5
Tb	-2.3	-6.1	-1.4	-10.3	-10.4
Dy	-8.9	-10.6	-5.1	-17.5	-16.7
Y	-9.0	-11.4	-5.1	-17.9	-17.2
Ho	-11.9	-15.1	-7.9	-24.5	-22.8
Er	-15.1	-20.1	-11.1	-31.7	-29.2
Tm	-17.9	-24.5	-14.1	-38.4	-35.1
Yb	-20.0	-28.1	-16.6	-43.5	-39.4
Lu	-23.1	-32.4	-20.6	-49.6	-44.7

are *Cmca* $X_2^-(0, a)$, *P4/ncc* $X_2^-(a, a)$, *Cmca* $M_5^+(a, 0)$, *Pbcn* $M_5^+(a, a)$, and *Pbca* $X_2^-(0, a) + M_5^+(b, 0)$. The calculated total energies of these five phases relative to their $I4/mcm$ phase is given in Table I.

For EuNiO_2 , which has only the X_2^- instability, just the $X_2^-(0, a)$ and $X_2^-(a, a)$ isotropy subgroups could be stabilized. They are degenerate within the numerical accuracy of my calculations. Correspondingly, the distortions from the $I4/mcm$ structures are also small. For example, the $X_2^-(0, a)$ phase exhibits a shear distortion of the Eu squares of 0.16° and a buckling of the O-Ni-O angles within the Ni-O squares of 0.11° .

Compounds with rare-earth ions smaller than Eu exhibit additional M_5^+ instability, and distortions due to this mode could be stabilized for these compounds. In GdNiO_3 , the $M_5^+(a, 0)$ and $M_5^+(a, a)$ phases are degenerate with the $I4/mcm$ phase within the numerical accuracy of the calculations. The $X_2^-(0, a)$ phase has the lowest energy with a relative energy of -2.8 meV/atom. This is close to that of the $X_2^-(a, a)$ and $X_2^-(0, a) + M_5^+(b, 0)$ phases, which have relative energies of -2.1 and -2.5 meV/atom, respectively. Such a near degeneracy in the calculated total energies indicates that there will be fluctuations among these structures at temperatures higher than corresponding to the energy scale of 0.7 meV/atom (≈ 8 K).

TbNiO_2 exhibits a qualitative change in the energetics of the structural distortions, with its $X_2^-(0, a) + M_5^+(b, 0)$ phase now having the lowest energy with a relative value of -10.4 meV/atom. Its $M_5^+(a, a)$ distortion has a slightly larger relative energy of -10.3 meV/atom. The larger energy gain is accompanied by a substantial in-

crease of structural distortions. For example, the Tb squares distort by 9.6° and 4.5° in the two phases, respectively. This is a large distinction between two structures that are so close in energy.

There is yet another qualitative change in the energetics of the structural distortions as the size of the rare-earth ion is decreased further. For the compounds with $R = \text{Dy-Lu}$, the $M_5^+(a, a)$ phase has the lowest energy, with the $X_2^-(0, a) + M_5^+(b, 0)$ phase lying above it in relative energy. The energy difference between the $M_5^+(a, a)$ and $X_2^-(0, a) + M_5^+(b, 0)$ phases is only 0.1 meV/atom for TbNiO_2 , and the difference remains below 2.0 meV/atom up to HoNiO_2 . The energy gap between these phases progressively increases to a value of 4.9 meV/atom for LuNiO_2 .

Hence, the two defining characteristics of the energetics of the structural distortions of the rare-earth infinite-layer nickelates is the presence of competing phases with similar energies and tunability of the order parameter of the lowest-energy phase as a function of the rare-earth ion size. Both these features imply that any structural transition that is possible due to the phonon instabilities present in these materials can be driven to 0 K.

Interestingly, calculations show that a related material LaNiO_3 exhibits similar structural degeneracies and is also in the vicinity of a structural quantum critical point, whereas YNiO_3 was proposed not to host any structural fluctuations [96]. Structural distortions in these materials occur due to the M_3^+ and R_4^+ phonon instabilities present in the parent cubic phase. It was argued that competing structural phases occur in LaNiO_3 due to a large difference in the imaginary frequencies between the unstable M_3^+ and R_4^+ modes, while a similar value of the imaginary frequency of these modes resulted in a large energy gain for the $Pnma$ structure with the $a^+b^-b^-$ tilt pattern in YNiO_3 . Therefore, a large difference between the calculated imaginary frequencies of two distinct phonon modes seems to lead to energetically competing structural distortions.

Does magnetic ordering change the energetics of the structural distortions?

Although magnetic ordering has not been experimentally observed in any of the infinite-layer rare-earth nickelates, DFT calculations find a small gain in energy when an antiferromagnetic solution is allowed, suggesting a weak tendency toward antiferromagnetism in these materials [42, 60, 63, 97]. Zhang *et al.* have shown that the phonon instability at the A point in the $P4/mmm$ phase is sensitive to the presence of antiferromagnetic order [80]. In particular, they find that the A_3^+ mode in NdNiO_2 , which is calculated to be stable in the non-spin-polarized phase, becomes unstable when the G-type antiferromagnetic solution is allowed. They are then able

TABLE II. Total energies of the five distortions due to the X_2^- and M_5^+ instabilities of the $I4/mcm$ phase in the presence of the G-type antiferromagnetic order. The energies are given relative to the respective antiferromagnetic $I4/mcm$ phase in the units of meV/atom. Note that the order parameters refer to that of the initial structures. Symmetry-allowed distortions appear for the final relaxed structures.

	<i>Cmca</i>	<i>P4/ncc</i>	<i>Cmca</i>	<i>Pbcn</i>	<i>Pbca</i>
	$X_2^-(0, a)$	$X_2^-(a, a)$	$M_5^+(a, 0)$	$M_5^+(a, a)$	$X_2^-(0, a)$ + $M_5^+(b, 0)$
RNiO ₂					
Eu	-0.3	-0.3	< -0.1	< -0.1	-0.4
Gd	-2.8	-4.1	-1.7	-10.9	-9.1
Tb	-5.3	-8.3	-4.2	-18.0	-15.3
Dy	-7.9	-12.4	-6.9	-24.8	-21.2
Y	-8.1	-12.8	-7.1	-24.5	-21.0
Ho	-10.6	-16.5	-9.9	-31.2	-26.8
Er	-13.7	-21.0	-13.5	-37.8	-32.7
Tm	-16.8	-24.9	-17.0	-43.8	-37.9
Yb	-19.4	-27.7	-20.2	-48.0	-41.5
Lu	-23.1	-31.3	-24.6	-53.2	-46.1

to stabilize the $I4/mcm$ phase for NdNiO_2 , as well as for compounds with Pr, Sm and smaller rare-earth ions. I was able to reproduce this result. In fact, I find the $I4/mcm$ phase to be lower in energy than the $P4/mmm$ phase for all RNiO_2 compounds except LaNiO_2 (*i.e.* $R = \text{Ce-Lu}$) when the G-type order is imposed. [Similar structural instability emerges also when the C-type order is allowed because the calculated energy difference between two antiferromagnetic states is less than 1.0 meV/Ni.] The calculated energy gain of the G-type $I4/mcm$ phase relative to the respective non-spin-polarized $P4/mmm$ phase ranges from 17.1 eV/atom for CeNiO_2 to 111.9 meV/atom for LuNiO_2 .

Zhang *et al.*'s results suggest that the inclusion of antiferromagnetic order can qualitatively change the energetics of the structural instabilities present in this family of compounds. I generated the minimal conventional unit cells that allow the G-type antiferromagnetic ordering for the five isotropy subgroups of the $I4/mcm$ phase stabilized above. I then fully relaxed these structures by minimizing the atomic forces and lattice stress in the presence of the antiferromagnetic order. As in the case of non-spin-polarized calculations discussed above, the compounds with $R = \text{Ce-Sm}$ relaxed back to the $I4/mcm$ phase also when the G-type antiferromagnetic solution was allowed. The energies of the rest of the compounds that could be stabilized in the antiferromagnetically ordered lower-symmetry phases are given in Table II relative to that of the respective antiferromagnetically ordered $I4/mcm$ phase.

I find the inclusion of the antiferromagnetic order marginally lowers (by few meV/atom or less) the relative energies of the five distorted structures. For EuNiO_2 , the $M_5^+(a, 0)$, $M_5^+(a, a)$, and $X_2^-(0, a) + M_5^+(b, 0)$ phases be-

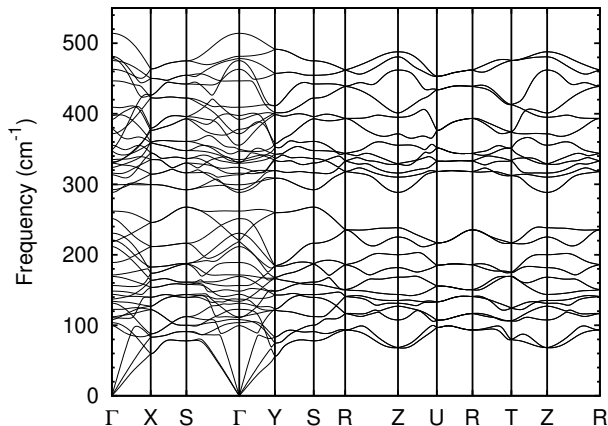


FIG. 7. Calculated non-spin-polarized phonon dispersions of fully-relaxed YNiO_2 in the $Pbcn$ phase corresponding to the $M_5^+(a, a)$ distortion of the $I4/mcm$ phase. The high-symmetry points are Γ $(0, 0, 0)$, X $(\frac{1}{2}, 0, 0)$, S $(\frac{1}{2}, \frac{1}{2}, 0)$, Y $(0, \frac{1}{2}, 0)$, R $(\frac{1}{2}, \frac{1}{2}, \frac{1}{2})$, Z $(0, 0, \frac{1}{2})$, U $(\frac{1}{2}, 0, \frac{1}{2})$, and T $(0, \frac{1}{2}, \frac{1}{2})$ in terms of the reciprocal lattice vectors.

come more stable than the $I4/mcm$ phase, which was not the case when a magnetic solution was not allowed. Otherwise, the structural energetics with antiferromagnetism is remarkably similar to that of the non-spin-polarized case. In particular, it still exhibits near-degenerate structures and a change in the order parameter of the lowest-lying phase as a function of the rare-earth ion. If these late rare-earth compounds also do not exhibit magnetic order like the early ones, this suggests that a structural quantum criticality occurs in the presence of magnetic fluctuations.

Are there other distortions with even lower energy?

In principle, the five low-symmetry structures that could be stabilized due to the X_2^- and M_5^+ unstable modes of the $I4/mcm$ phase may yet exhibit structural instabilities. I did not have the computational resources to calculate the phonon dispersions of all the low-symmetry phases of the ten compounds with $R = \text{Eu-Lu}$ for which these structures could be stabilized. Nevertheless, I calculated the phonon dispersions of YNiO_2 in its lowest-energy $Pbcn$ $M_5^+(a, a)$ phase, which is shown in Fig. 7. This phase does not exhibit any unstable phonon modes, implying that it is dynamically stable. Since $Pbcn$ $M_5^+(a, a)$ phase is the lowest-energy structure for the compounds with $R = \text{Dy-Lu}$, there are unlikely to be other lower-energy distortions that can be continuously connected to the parent $P4/mmm$ phase via phonon instabilities.

Carrasco Álvarez *et al.* have argued using first principles calculations that the $Pbnm$ structure with a $a^-a^-c^+$

tilt pattern of the NiO_4 square is the ground state phase of the infinite-layer nickelates with smaller rare-earth ions [79]. I tried to be able to stabilize this phase for YNiO_2 on a $2 \times 2 \times 2$ supercell of the $P4/mmm$ structure and was able to do so only when antiferromagnetism was allowed. This is again suggestive of the strong coupling between magnetism and structural instabilities in these materials [80]. The fully relaxed $Pbnm$ $a^-a^-c^+$ structure also exhibits the antipolar motion of the R ions, as found by Carrasco Álvarez *et al.* I obtain a value of 65.5 meV/atom for the calculated energy gain of the $Pbnm$ $a^-a^-c^+$ phase relative to the $P4/mmm$ phase when the C-type antiferromagnetic order is imposed in both phases. For comparison, the energy gain of the $M_5^+(a, a)$ distortion of the $I4/mcm$ phase relative to the $P4/mmm$ phase for the C-type antiferromagnetic state is 74.2 meV/atom. Therefore, the $Pbnm$ $a^-a^-c^+$ structure is likely not the ground state phase of the infinite-layer nickelates with small rare-earth ions.

SUMMARY AND CONCLUSIONS

In summary, I have investigated the energetics of the structural distortions of the infinite-layer rare-earth nickelates and find that these materials may lie near a structural quantum critical point. I first confirmed the previous results showing the parent $P4/mmm$ phase of the $R = \text{Sm-Lu}$ compounds to be unstable towards the $I4/mcm$ phase due to an A_3^+ phonon instability [77, 78, 80]. I then calculated the non-spin-polarised phonon dispersions of the $R = \text{Sm-Lu}$ compounds in the $I4/mcm$ phase. Only SmNiO_2 is dynamically stable in this structure. GdNiO_2 exhibits an X_2^- instability, while the rest exhibit an additional M_5^+ instability. I used group-theoretical analysis to identify all twelve isotropy subgroups that are possible due these two instabilities and generated distorted structures corresponding to their order parameters. After full structural relaxations minimizing both the atomic forces and lattice stresses, only five isotropy subgroups corresponding to the $Cmca$ $X_2^-(0, a)$, $P4/ncc$ $X_2^-(a, a)$, $Cmca$ $M_5^+(a, 0)$, $Pbcn$ $M_5^+(a, a)$, and $Pbca$ $X_2^-(0, a) + M_5^+(b, 0)$ order parameters could be stabilized.

From the non-spin-polarized calculations, the $M_5^+(a, a)$ phase has the lowest energy for the smallest rare-earth compound LuNiO_2 relative to its $I4/mcm$ phase. Its $X_2^-(0, a) + M_5^+(b, 0)$ phase is higher in energy than the $M_5^+(a, a)$ phase by 4.9 meV/atom. The energy difference between these two phases decreases as the rare-earth ion size is increased, reaching a value of less than 2.0 meV/atom for compounds with $R = \text{Ho}$ or smaller. There is a qualitative change in the energetics for TbNiO_2 , which now has the $X_2^-(0, a) + M_5^+(b, 0)$ phase lower in energy than the $M_5^+(a, a)$ phase, albeit only by 0.1 meV/atom. The energetics shuffle again for

GdNiO₂. Its lowest-energy phase is $X_2^-(0, a)$, and it is only 0.4 and 0.7 meV/atom higher in energy than the $X_2^-(0, a) + M_5^+(b, 0)$ and $X_2^-(a, a)$ phases, respectively.

The near degeneracy of the phases corresponding to distinct structural order parameters and the tunability of the relative energies of these competing phases both suggest that any structural transition that might occur due to the phonon instabilities present in the $I4/mcm$ phase of these materials can be suppressed to 0 K. I find the inclusion of the nearest-neighbor antiferromagnetic order only lowers the relative energy of the low-symmetry phases by few meV/atom. In particular, the qualitative and quantitative aspects of the competition between different order parameters remains. If the infinite-layer nickelates with smaller rare-earth ions do not exhibit magnetic ordering like those with the larger ones, this implies that the proximity to the structural quantum criticality occurs in the presence of magnetic fluctuations.

Recent experiments on $(\text{Ca}_x\text{Sr}_{1-x})_3\text{Rh}_4\text{Sn}_{13}$, $(\text{Ca}_x\text{Sr}_{1-x})_3\text{Ir}_4\text{Sn}_{13}$, and $\text{LaCu}_{6-x}\text{Au}_x$ show these materials to host a structural quantum critical point, which manifests as a softening of the associated phonon modes at $T \rightarrow 0$ K [98–102]. The measured heat capacity is strongly enhanced near the critical point due to the ensuing preponderance of the phonon density of states. Similar softening of the X_2^- and M_5^+ phonon modes and enhancement of the heat capacity will be the experimental consequences of the structural quantum criticality proposed here for the infinite-layer nickelates. Moreover, superconducting T_c is found to peak near the quantum critical point in $(\text{Ca}_x\text{Sr}_{1-x})_3\text{Ir}_4\text{Sn}_{13}$ [103], and the infinite-layer nickelates should exhibit similar enhancement if phonons play an important role in their superconductivity.

ACKNOWLEDGEMENTS

This work was supported by GENCI-TGCC under grant no. A0110913028.

[1] D. Li, K. Lee, B. Y. Wang, M. Osada, S. Crossley, H. R. Lee, Y. Cui, Y. Hikita, and H. Y. Hwang, Superconductivity in an infinite-layer nickelate, *Nature* **572**, 624 (2019).

[2] M. Osada, B. Y. Wang, B. H. Goodge, K. Lee, H. Yoon, K. Sakuma, D. Li, M. Miura, L. F. Kourkoutis, and H. Y. Hwang, A superconducting praseodymium nickelate with infinite layer structure, *Nano Lett.* **20**, 5735 (2020).

[3] M. Osada, B. Y. Wang, B. H. Goodge, S. P. Harvey, K. Lee, D. Li, L. F. Kourkoutis, and H. Y. Hwang, Nickelate superconductivity without rare-earth magnetism: $(\text{La}, \text{Sr})\text{NiO}_2$, *Adv. Mater.* **33**, 2104083 (2021).

[4] S. Zeng, C. Li, L. E. Chow, Y. Cao, Z. Zhang, C. S. Tang, X. Yin, Z. S. Lim, J. Hu, P. Yang, *et al.*, Superconductivity in infinite-layer nickelate $\text{La}_{1-x}\text{Ca}_x\text{NiO}_2$ thin films, *Sci. Adv.* **8**, eabl9927 (2022).

[5] M. Hepting, D. Li, C. Jia, H. Lu, E. Paris, Y. Tseng, X. Feng, M. Osada, E. Been, Y. Hikita, *et al.*, Electronic structure of the parent compound of superconducting infinite-layer nickelates, *Nat. Mater.* **19**, 381 (2020).

[6] Q. Li, C. He, J. Si, X. Zhu, Y. Zhang, and H.-H. Wen, Absence of superconductivity in bulk $\text{Nd}_{1-x}\text{Sr}_x\text{NiO}_2$, *Communications Materials* **1**, 1 (2020).

[7] Y. Fu, L. Wang, H. Cheng, S. Pei, X. Zhou, J. Chen, S. Wang, R. Zhao, W. Jiang, C. Liu, *et al.*, Core-level x-ray photoemission and Raman spectroscopy studies on electronic structures in Mott-Hubbard type nickelate oxide NdNiO_2 , arXiv preprint arXiv:1911.03177 (2019).

[8] K. Lee, B. H. Goodge, D. Li, M. Osada, B. Y. Wang, Y. Cui, L. F. Kourkoutis, and H. Y. Hwang, Aspects of the synthesis of thin film superconducting infinite-layer nickelates, *Apl Mater.* **8**, 041107 (2020).

[9] D. Li, B. Y. Wang, K. Lee, S. P. Harvey, M. Osada, B. H. Goodge, L. F. Kourkoutis, and H. Y. Hwang, Superconducting dome in $\text{Nd}_{1-x}\text{Sr}_x\text{NiO}_2$ infinite layer films, *Phys. Rev. Lett.* **125**, 027001 (2020).

[10] S. Zeng, C. S. Tang, X. Yin, C. Li, M. Li, Z. Huang, J. Hu, W. Liu, G. J. Omar, H. Jani, *et al.*, Phase diagram and superconducting dome of infinite-layer $\text{Nd}_{1-x}\text{Sr}_x\text{NiO}_2$ thin films, *Phys. Rev. Lett.* **125**, 147003 (2020).

[11] B. H. Goodge, D. Li, K. Lee, M. Osada, B. Y. Wang, G. A. Sawatzky, H. Y. Hwang, and L. F. Kourkoutis, Doping evolution of the Mott-Hubbard landscape in infinite-layer nickelates, *Proceedings of the National Academy of Sciences* **118** (2021).

[12] B.-X. Wang, H. Zheng, E. Kriviyakina, O. Chmaissem, P. P. Lopes, J. W. Lynn, L. C. Gallington, Y. Ren, S. Rosenkranz, J. Mitchell, *et al.*, Synthesis and characterization of bulk $\text{Nd}_{1-x}\text{Sr}_x\text{NiO}_2$ and $\text{Nd}_{1-x}\text{Sr}_x\text{NiO}_3$, *Physical review materials* **4**, 084409 (2020).

[13] Q. Gu, Y. Li, S. Wan, H. Li, W. Guo, H. Yang, Q. Li, X. Zhu, X. Pan, Y. Nie, *et al.*, Single particle tunneling spectrum of superconducting $\text{Nd}_{1-x}\text{Sr}_x\text{NiO}_2$ thin films, *Nat. Commun.* **11**, 1 (2020).

[14] B. Y. Wang, D. Li, B. H. Goodge, K. Lee, M. Osada, S. P. Harvey, L. F. Kourkoutis, M. R. Beasley, and H. Y. Hwang, Isotropic Pauli-limited superconductivity in the infinite-layer nickelate $\text{Nd}_{0.775}\text{Sr}_{0.225}\text{NiO}_2$, *Nat. Phys.* **17**, 473 (2021).

[15] Y. Xiang, Q. Li, Y. Li, H. Yang, Y. Nie, and H.-H. Wen, Physical properties revealed by transport measurements for superconducting $\text{Nd}_{0.8}\text{Sr}_{0.2}\text{NiO}_2$ thin films, *Chinese Physics Letters* **38**, 047401 (2021).

[16] M. Osada, B. Y. Wang, K. Lee, D. Li, and H. Y. Hwang, Phase diagram of infinite layer praseodymium nickelate $\text{Pr}_{1-x}\text{Sr}_x\text{NiO}_2$ thin films, *Phys. Rev. Materials* **4**, 121801 (2020).

[17] M. Rossi, H. Lu, A. Nag, D. Li, M. Osada, K. Lee, B. Y. Wang, S. Agrestini, M. Garcia-Fernandez, J. Kas, *et al.*, Orbital and spin character of doped carriers in infinite-layer nickelates, *Physical Review B* **104**, L220505 (2021).

[18] Y. Cui, C. Li, Q. Li, X. Zhu, Z. Hu, Y.-f. Yang, J. Zhang, R. Yu, H.-H. Wen, and W. Yu, NMR evidence of antiferromagnetic spin fluctuations in $\text{Nd}_{0.85}\text{Sr}_{0.15}\text{NiO}_2$,

- Chinese Physics Letters **38**, 067401 (2021).
- [19] C. He, X. Ming, Q. Li, X. Zhu, J. Si, and H.-H. Wen, Synthesis and physical properties of perovskite $\text{sm}1\text{-xsr}x\text{NiO}_3$ ($x = 0, 0.2$) and infinite-layer $\text{sm}0.8\text{sr}0.2\text{nio}2$ nickelates, *Journal of Physics: Condensed Matter* **33**, 265701 (2021).
- [20] R. Ortiz, H. Menke, F. Misják, D. Mantadakis, K. Fürsich, E. Schierle, G. Logvenov, U. Kaiser, B. Keimer, P. Hansmann, *et al.*, Superlattice approach to doping infinite-layer nickelates, *Physical Review B* **104**, 165137 (2021).
- [21] Q. Gao, Y. Zhao, X.-J. Zhou, and Z. Zhu, Preparation of Superconducting Thin Films of Infinite-Layer Nickelate $\text{Nd}_{0.8}\text{Sr}_{0.2}\text{NiO}_2$, *Chinese Physics Letters* **38**, 077401 (2021).
- [22] S. Zeng, X. Yin, C. Li, L. Chow, C. Tang, K. Han, Z. Huang, Y. Cao, D. Wan, Z. Zhang, *et al.*, Observation of perfect diamagnetism and interfacial effect on the electronic structures in infinite layer $\text{Nd}_{0.8}\text{Sr}_{0.2}\text{NiO}_2$ superconductors, *Nat. Commun.* **13**, 1 (2022).
- [23] X.-R. Zhou, Z.-X. Feng, P.-X. Qin, H. Yan, X.-N. Wang, P. Nie, H.-J. Wu, X. Zhang, H.-Y. Chen, Z.-A. Meng, *et al.*, Negligible oxygen vacancies, low critical current density, electric-field modulation, in-plane anisotropic and high-field transport of a superconducting $\text{Nd}_{0.8}\text{Sr}_{0.2}\text{NiO}_2/\text{SrTiO}_3$ heterostructure, *Rare Metals* **40**, 2847 (2021).
- [24] D. Zhao, Y. Zhou, Y. Fu, L. Wang, X. Zhou, H. Cheng, J. Li, D. Song, S. Li, B. Kang, *et al.*, Intrinsic Spin Susceptibility and Pseudogaplike Behavior in Infinite-Layer LaNiO_2 , *Physical Review Letters* **126**, 197001 (2021).
- [25] H. Lin, D. J. Gawryluk, Y. M. Klein, S. Huangfu, E. Pomjakushina, F. von Rohr, and A. Schilling, Universal spin-glass behaviour in bulk LaNiO_2 , PrNiO_2 and NdNiO_2 , *New Journal of Physics* **24**, 013022 (2022).
- [26] Y.-T. Hsu, B. Y. Wang, M. Berben, D. Li, K. Lee, C. Duffy, T. Ottenbros, W. J. Kim, M. Osada, S. Wiedmann, *et al.*, Insulator-to-metal crossover near the edge of the superconducting dome in $\text{Nd}_{1-x}\text{Sr}_x\text{NiO}_2$, *Physical Review Research* **3**, L042015 (2021).
- [27] H. Lu, M. Rossi, A. Nag, M. Osada, D. Li, K. Lee, B. Wang, M. Garcia-Fernandez, S. Agrestini, Z. Shen, *et al.*, Magnetic excitations in infinite-layer nickelates, *Science* **373**, 213 (2021).
- [28] Y. Li, W. Sun, J. Yang, X. Cai, W. Guo, Z. Gu, Y. Zhu, and Y. Nie, Impact of cation stoichiometry on the crystalline structure and superconductivity in nickelates, *arXiv preprint arXiv:2106.02485* (2021).
- [29] P. Puphal, Y.-M. Wu, K. Fürsich, H. Lee, M. Pakdaman, J. A. Bruin, J. Nuss, Y. E. Suyolcu, P. A. van Aken, B. Keimer, *et al.*, Topotactic transformation of single crystals: From perovskite to infinite-layer nickelates, *Science advances* **7**, eabl8091 (2021).
- [30] Z. Chen, M. Osada, D. Li, E. M. Been, S.-D. Chen, M. Hashimoto, D. Lu, S.-K. Mo, K. Lee, B. Y. Wang, *et al.*, Electronic structure of superconducting nickelates probed by resonant photoemission spectroscopy, *Matter* (2022).
- [31] N. N. Wang, M. W. Yang, K. Y. Chen, Z. Yang, H. Zhang, Z. H. Zhu, Y. Uwatoko, X. L. Dong, K. J. Jin, J. P. Sun, *et al.*, Pressure-induced monotonic enhancement of T_c to over 30 k in the superconducting $\text{Pr}_{0.82}\text{Sr}_{0.18}\text{NiO}_2$ thin films, *arXiv preprint arXiv:2109.12811* (2021).
- [32] X. Zhou, X. Zhang, J. Yi, P. Qin, Z. Feng, P. Jiang, Z. Zhong, H. Yan, X. Wang, H. Chen, *et al.*, Antiferromagnetism in ni-based superconductors, *Advanced Materials* **34**, 2106117 (2022).
- [33] R. Ortiz, P. Puphal, M. Klett, F. Hotz, R. Kremer, H. Trepka, M. Hemmida, H.-A. K. von Nidda, M. Isobe, R. Khasanov, *et al.*, Magnetic correlations in infinite-layer nickelates: an experimental and theoretical multi-method study, *arXiv preprint arXiv:2111.13668* (2021).
- [34] M. Rossi, M. Osada, J. Choi, S. Agrestini, D. Jost, Y. Lee, H. Lu, B. Y. Wang, K. Lee, A. Nag, *et al.*, A broken translational symmetry state in an infinite-layer nickelate, *arXiv preprint arXiv:2112.02484* (2021).
- [35] G. Krieger, L. Martinelli, S. Zeng, L. Chow, K. Kummer, R. Arpaia, M. M. Sala, N. Brookes, A. Ariando, N. Viart, *et al.*, Charge and spin order dichotomy in ndnio_2 driven by $\text{sr}t\text{io}_3$ capping layer, *arXiv preprint arXiv:2112.03341* (2021).
- [36] C. C. Tam, J. Choi, X. Ding, S. Agrestini, A. Nag, B. Huang, H. Luo, M. García-Fernández, L. Qiao, and K.-J. Zhou, Charge density waves in infinite-layer NdNiO_2 nickelates, *arXiv preprint arXiv:2112.04440* (2021).
- [37] B. H. Goodge, B. Geisler, K. Lee, M. Osada, B. Y. Wang, D. Li, H. Y. Hwang, R. Pentcheva, and L. F. Kourkoutis, Reconstructing the polar interface of infinite-layer nickelate thin films, *arXiv preprint arXiv:2201.03613* (2022).
- [38] L. E. Chow, S. K. Sudheesh, P. Nandi, S. Zeng, Z. Zhang, X. Du, Z. S. Lim, E. E. Chia, and A. Ariando, Pairing symmetry in infinite-layer nickelate superconductor, *arXiv preprint arXiv:2201.10038* (2022).
- [39] J. Fowlie, M. Hadjimichael, M. M. Martins, D. Li, M. Osada, B. Y. Wang, K. Lee, Y. Lee, Z. Salman, T. Prokscha, *et al.*, Intrinsic magnetism in superconducting infinite-layer nickelates, *arXiv preprint arXiv:2201.11943* (2022).
- [40] S. P. Harvey, B. Y. Wang, J. Fowlie, M. Osada, K. Lee, Y. Lee, D. Li, and H. Y. Hwang, Evidence for nodal superconductivity in infinite-layer nickelates, *arXiv preprint arXiv:2201.12971* (2022).
- [41] X. Ding, S. Shen, H. Leng, M. Xu, Y. Zhao, J. Zhao, X. Sui, X. Wu, H. Xiao, X. Zu, *et al.*, Stability of Superconducting $\text{Nd}_{0.8}\text{Sr}_{0.2}\text{NiO}_2$ Thin Films, *arXiv preprint arXiv:2201.13032* (2022).
- [42] A. S. Botana and M. R. Norman, Similarities and differences between LaNiO_2 and CaCuO_2 and implications for superconductivity, *Phys. Rev. X* **10**, 011024 (2020).
- [43] H. Sakakibara, H. Usui, K. Suzuki, T. Kotani, H. Aoki, and K. Kuroki, Model construction and a possibility of cupratelike pairing in a new d_9 nickelate superconductor (nd, sr) nio_2 , *Physical Review Letters* **125**, 077003 (2020).
- [44] M. Jiang, M. Berciu, and G. A. Sawatzky, Critical nature of the ni spin state in doped NdNiO_2 , *Phys. Rev. Lett.* **124**, 207004 (2020).
- [45] X. Wu, D. Di Sante, T. Schwemmer, W. Hanke, H. Y. Hwang, S. Raghu, and R. Thomale, Robust $d_{x^2-y^2}$ -wave superconductivity of infinite-layer nickelates, *Phys. Rev. B* **101**, 060504 (2020).
- [46] Y. Nomura, M. Hirayama, T. Tadano, Y. Yoshimoto, K. Nakamura, and R. Arita, Formation of a two-dimensional single-component correlated electron system and band engineering in the nickelate superconduc-

- tor ndnio 2, *Physical Review B* **100**, 205138 (2019).
- [47] S. Ryee, H. Yoon, T. J. Kim, M. Y. Jeong, and M. J. Han, Induced magnetic two-dimensionality by hole doping in the superconducting infinite-layer nickelate $\text{Nd}_{1-x}\text{Sr}_x\text{NiO}_2$, *Physical Review B* **101**, 064513 (2020).
- [48] H. Zhang, L. Jin, S. Wang, B. Xi, X. Shi, F. Ye, and J.-W. Mei, Effective hamiltonian for nickelate oxides $\text{Nd}_{1-x}\text{Sr}_x\text{NiO}_2$, *Physical Review Research* **2**, 013214 (2020).
- [49] G.-M. Zhang, Y.-F. Yang, and F.-C. Zhang, Self-doped Mott insulator for parent compounds of nickelate superconductors, *Physical Review B* **101**, 020501(R) (2020).
- [50] Y.-H. Zhang and A. Vishwanath, Type-II $t - J$ model in superconducting nickelate $\text{Nd}_{1-x}\text{Sr}_x\text{NiO}_2$, *Physical Review Research* **2**, 023112 (2020).
- [51] P. Jiang, L. Si, Z. Liao, and Z. Zhong, Electronic structure of rare-earth infinite-layer $R\text{NiO}_2$ ($R = \text{La}, \text{Nd}$), *Physical Review B* **100**, 201106 (2019).
- [52] P. Werner and S. Hoshino, Nickelate superconductors: Multiorbital nature and spin freezing, *Physical Review B* **101**, 041104 (2020).
- [53] L.-H. Hu and C. Wu, Two-band model for magnetism and superconductivity in nickelates, *Physical Review Research* **1**, 032046 (2019).
- [54] T. Zhou, Y. Gao, and Z. Wang, Spin excitations in nickelate superconductors, *Science China Physics, Mechanics & Astronomy* **63**, 1 (2020).
- [55] F. Bernardini, V. Olevano, and A. Cano, Magnetic penetration depth and T_c in superconducting nickelates, *Physical Review Research* **2**, 013219 (2020).
- [56] Y. Gu, S. Zhu, X. Wang, J. Hu, and H. Chen, A substantial hybridization between correlated Ni- d orbital and itinerant electrons in infinite-layer nickelates, *Communications Physics* **3**, 1 (2020).
- [57] M.-Y. Choi, K.-W. Lee, and W. E. Pickett, Role of $4f$ states in infinite-layer NdNiO_2 , *Physical Review B* **101**, 020503 (2020).
- [58] F. Lechermann, Late transition metal oxides with infinite-layer structure: Nickelates versus cuprates, *Physical Review B* **101**, 081110 (2020).
- [59] J. Chang, J. Zhao, and Y. Ding, Hund-heisenberg model in superconducting infinite-layer nickelates, *The European Physical Journal B* **93**, 1 (2020).
- [60] Z. Liu, Z. Ren, W. Zhu, Z. Wang, and J. Yang, Electronic and magnetic structure of infinite-layer NdNiO_2 : trace of antiferromagnetic metal, *npj Quantum Materials* **5**, 1 (2020).
- [61] J. Karp, A. S. Botana, M. R. Norman, H. Park, M. Zingl, and A. Millis, Many-body electronic structure of NdNiO_2 and CaCuO_2 , *Physical Review X* **10**, 021061 (2020).
- [62] M. Kitatani, L. Si, O. Janson, R. Arita, Z. Zhong, and K. Held, Nickelate superconductors—a renaissance of the one-band hubbard model, *npj Quantum Materials* **5**, 1 (2020).
- [63] E. Been, W.-S. Lee, H. Y. Hwang, Y. Cui, J. Zaanen, T. Devereaux, B. Moritz, and C. Jia, Electronic structure trends across the rare-earth series in superconducting infinite-layer nickelates, *Phys. Rev. X* **11**, 011050 (2021).
- [64] I. Leonov, S. Skornyakov, and S. Savrasov, Lifshitz transition and frustration of magnetic moments in infinite-layer NdNiO_2 upon hole doping, *Physical Review B* **101**, 241108 (2020).
- [65] F. Lechermann, Multiorbital processes rule the $\text{Nd}_{1-x}\text{Sr}_x\text{NiO}_2$ normal state, *Physical Review X* **10**, 041002 (2020).
- [66] M.-Y. Choi, W. E. Pickett, and K.-W. Lee, Fluctuation-frustrated flat band instabilities in NdNiO_2 , *Physical Review Research* **2**, 033445 (2020).
- [67] Y. Wang, C.-J. Kang, H. Miao, and G. Kotliar, Hund’s metal physics: From SrNiO_2 to LaNiO_2 , *Physical Review B* **102**, 161118 (2020).
- [68] B. Kang, C. Melnick, P. Semon, S. Ryee, M. J. Han, G. Kotliar, and S. Choi, Infinite-layer nickelates as ni-egund’s metals, arXiv preprint arXiv:2007.14610 (2020).
- [69] J. Kapeghian and A. S. Botana, Electronic structure and magnetism in infinite-layer nickelates $R\text{NiO}_2$ ($R = \text{La-Lu}$), *Physical Review B* **102**, 205130 (2020).
- [70] C.-J. Kang and G. Kotliar, Optical properties of the infinite-layer $\text{La}_{1-x}\text{Sr}_x\text{NiO}_2$ and hidden Hund’s physics, *Physical review letters* **126**, 127401 (2021).
- [71] R. Zhang, C. Lane, B. Singh, J. Nokelainen, B. Barbiellini, R. S. Markiewicz, A. Bansil, and J. Sun, Magnetic and f -electron effects in LaNiO_2 and NdNiO_2 nickelates with cuprate-like $3d_{x^2-y^2}$ band, *Communications Physics* **4**, 1 (2021).
- [72] F. Lechermann, Doping-dependent character and possible magnetic ordering of NdNiO_2 , *Physical Review Materials* **5**, 044803 (2021).
- [73] V. M. Katukuri, N. A. Bogdanov, O. Weser, J. Van den Brink, and A. Alavi, Electronic correlations and magnetic interactions in infinite-layer ndnio 2, *Physical Review B* **102**, 241112(R) (2020).
- [74] O. I. Malyi, J. Varignon, and A. Zunger, Bulk NdNiO_2 is thermodynamically unstable with respect to decomposition while hydrogenation reduces the instability and transforms it from metal to insulator, *Physical Review B* **105**, 014106 (2022).
- [75] T. Plienbumrung, M. T. Schmid, M. Daghofer, and A. M. Oleś, Character of doped holes in $\text{nd1-x}\text{srxnio2}$, *Condensed Matter* **6**, 33 (2021).
- [76] M. Klett, P. Hansmann, and T. Schäfer, Magnetic properties and pseudogap formation in infinite-layer nickelates: insights from the single-band Hubbard model, *Frontiers in Physics* , 45 (2022).
- [77] C. Xia, J. Wu, Y. Chen, and H. Chen, Dynamical structural instability and a new crystal-electronic structure of infinite-layer nickelates, arXiv preprint arXiv:2110.12405 (2021).
- [78] F. Bernardini, A. Bosin, and A. Cano, Geometric effects in the infinite-layer nickelates, arXiv preprint arXiv:2110.13580 (2021).
- [79] Á. A. Carrasco Álvarez, S. Petit, L. Iglesias, W. Prellier, M. Bibes, and J. Varignon, Structural instabilities of infinite-layer nickelates from first-principles simulations, arXiv preprint arXiv:2112.02642 (2021).
- [80] Y. Zhang, J. Zhang, X. He, J. Wang, and P. Ghosez, Phase Diagram of Infinite-layer Nickelate Compounds from First- and Second-principles Calculations, arXiv preprint arXiv:2201.00709 (2022).
- [81] J. Karp, A. Hampel, and A. J. Millis, Superconductivity and Antiferromagnetism in NdNiO_2 and CaCuO_2 : A Cluster DMFT Study, arXiv preprint arXiv:2201.10481 (2022).
- [82] M. Jiang, Characterizing the superconducting instability in a two-orbital d - s model: insights to

- infinite-layer nickelate superconductors, arXiv preprint arXiv:2201.12967 (2022).
- [83] L. Si, W. Xiao, J. Kaufmann, J. M. Tomczak, Y. Lu, Z. Zhong, and K. Held, Topotactic hydrogen in nickelate superconductors and akin infinite-layer oxides $\text{A} \text{B} \text{O}_2$, *Physical Review Letters* **124**, 166402 (2020).
- [84] M. Crespin, P. Levitz, and L. Gataineau, Reduced forms of lanio 3 perovskite. part 1.—evidence for new phases: $\text{La}_2\text{Ni}_2\text{O}_5$ and lanio 2, *Journal of the Chemical Society, Faraday Transactions 2: Molecular and Chemical Physics* **79**, 1181 (1983).
- [85] P. Levitz, M. Crespin, and L. Gataineau, Reduced forms of lanio 3 perovskite. part 2.—x-ray structure of lanio 2 and extended x-ray absorption fine structure study: local environment of monovalent nickel, *Journal of the Chemical Society, Faraday Transactions 2: Molecular and Chemical Physics* **79**, 1195 (1983).
- [86] M. Hayward, M. Green, M. Rosseinsky, and J. Sloan, Sodium hydride as a powerful reducing agent for topotactic oxide deintercalation: synthesis and characterization of the nickel (i) oxide lanio2, *Journal of the American Chemical Society* **121**, 8843 (1999).
- [87] M. Hayward and M. Rosseinsky, Synthesis of the infinite layer ni (i) phase NdNiO_{2+x} by low temperature reduction of NdNiO_3 with sodium hydride, *Solid state sciences* **5**, 839 (2003).
- [88] S. Baroni, S. de Gironcoli, A. Dal Corso, and P. Giannozzi, Phonons and related crystal properties from density-functional perturbation theory, *Rev. Mod. Phys.* **73**, 515 (2001).
- [89] P. Giannozzi, S. Baroni, N. Bonini, M. Calandra, R. Car, C. Cavazzoni, D. Ceresoli, G. L. Chiarotti, M. Cococcioni, I. Dabo, *et al.*, QUANTUM ESPRESSO: a modular and open-source software project for quantum simulations of materials, *J. Phys.: Condens. Matter* **21**, 395502 (2009).
- [90] A. Dal Corso, Pseudopotentials periodic table: From H to Pu, *Computational Materials Science* **95**, 337 (2014).
- [91] J. P. Perdew, K. Burke, and M. Ernzerhof, Generalized Gradient Approximation Made Simple, *Phys. Rev. Lett.* **77**, 3865 (1996).
- [92] H. T. Stokes, B. J. Campbell, and D. M. Hatch, ISOTROPY software suite, iso.byu.edu.
- [93] G. Kresse and J. Furthmüller, Efficient iterative schemes for *ab initio* total-energy calculations using a plane-wave basis set, *Physical review B* **54**, 11169 (1996).
- [94] H. T. Stokes and D. M. Hatch, FINDSYM: program for identifying the space-group symmetry of a crystal, *Journal of Applied Crystallography* **38**, 237 (2005).
- [95] A. Togo and I. Tanaka, SPGLIB: a software library for crystal symmetry search, arXiv preprint arXiv:1808.01590 (2018).
- [96] A. Subedi, Breathing distortions in the metallic, antiferromagnetic phase of lanio -_3 , *SciPost Physics* **5**, 020 (2018).
- [97] K.-W. Lee and W. E. Pickett, Infinite-layer LaNiO_2 : Ni^{1+} is not Cu^{2+} , *Physical Review B* **70**, 165109 (2004).
- [98] S. K. Goh, D. A. Tompsett, P. J. Saines, H. C. Chang, T. Matsumoto, M. Imai, K. Yoshimura, and F. M. Grosche, Ambient pressure structural quantum critical point in the phase diagram of $(\text{Ca}_x\text{Sr}_{1-x})_3\text{Rh}_4\text{Sn}_{13}$, *Physical review letters* **114**, 097002 (2015).
- [99] W. C. Yu, Y. W. Cheung, P. J. Saines, M. Imai, T. Matsumoto, C. Michioka, K. Yoshimura, and S. K. Goh, Strong Coupling Superconductivity in the Vicinity of the Structural Quantum Critical Point in $(\text{Ca}_x\text{Sr}_{1-x})_3\text{Rh}_4\text{Sn}_{13}$, *Physical review letters* **115**, 207003 (2015).
- [100] Y. Hu, Y. Cheung, W. Yu, M. Imai, H. Kanagawa, J. Murakawa, K. Yoshimura, and S. K. Goh, Soft phonon modes in the vicinity of the structural quantum critical point, *Physical Review B* **95**, 155142 (2017).
- [101] Y. W. Cheung, Y. J. Hu, M. Imai, Y. Tanioku, H. Kanagawa, J. Murakawa, K. Moriyama, W. Zhang, K. T. Lai, K. Yoshimura, *et al.*, Evidence of a structural quantum critical point in $(\text{Ca}_x\text{Sr}_{1-x})_3\text{Rh}_4\text{Sn}_{13}$ from a lattice dynamics study, *Physical Review B* **98**, 161103 (2018).
- [102] L. Poudel, A. F. May, M. R. Koehler, M. A. McGuire, S. Mukhopadhyay, S. Calder, R. E. Baumbach, R. Mukherjee, D. Sapkota, C. de la Cruz, *et al.*, Candidate Elastic Quantum Critical Point in $\text{LaCu}_{6-x}\text{Au}_x$, *Physical review letters* **117**, 235701 (2016).
- [103] P. K. Biswas, Z. Guguchia, R. Khasanov, M. Chinotti, L. Li, K. Wang, C. Petrovic, and E. Morenzoni, Strong enhancement of *s*-wave superconductivity near a quantum critical point of $\text{Ca}_3\text{Ir}_4\text{Sn}_{13}$, *Physical Review B* **92**, 195122 (2015).